Korean Journal of Radiology

KJR

Check for updates

Preoperative MRI Features Associated With Axillary Nodal Burden and Disease-Free Survival in Patients With Early-Stage Breast Cancer

Junjie Zhang[1]*, Zhi Yin[2]*, Jianxin Zhang[1], Ruirui Song[1], Yanfen Cui[1], Xiaotang Yang[1]

[1]Cancer Hospital Affiliated to Shanxi Medical University/Shanxi Province Cancer Hospital/Shanxi Hospital Affiliated to Cancer Hospital, Chinese Academy of Medical Sciences, Taiyuan, China
[2]College of Medical Imaging, Shanxi Medical University, Taiyuan, China

Objective: To investigate the potential association among preoperative breast MRI features, axillary nodal burden (ANB), and disease-free survival (DFS) in patients with early-stage breast cancer.
Materials and Methods: We retrospectively reviewed 297 patients with early-stage breast cancer (cT1-2N0M0) who underwent preoperative MRI between December 2016 and December 2018. Based on the number of positive axillary lymph nodes (LNs) determined by postoperative pathology, the patients were divided into high nodal burden (HNB; ≥3 positive LNs) and non-HNB (<3 positive LNs) groups. Univariable and multivariable logistic regression analyses were performed to identify independent risk factors associated with ANB. Predictive efficacy was evaluated using the receiver operating characteristic (ROC) curve and area under the curve (AUC). Univariable and multivariable Cox proportional hazards regression analyses were performed to determine preoperative features associated with DFS.
Results: We included 47 and 250 patients in the HNB and non-HNB groups, respectively. Multivariable logistic regression analysis revealed that multifocality/multicentricity (adjusted odds ratio [OR] = 3.905, 95% confidence interval [CI]: 1.685–9.051, P = 0.001) and peritumoral edema (adjusted OR = 3.734, 95% CI: 1.644–8.479, P = 0.002) were independent risk factors for HNB. Combined peritumoral edema and multifocality/multicentricity achieved an AUC of 0.760 (95% CI: 0.707–0.807) for predicting HNB, with a sensitivity and specificity of 83.0% and 63.2%, respectively. During the median follow-up period of 45 months (range, 5–61 months), 26 cases (8.75%) of breast cancer recurrence were observed. Multivariable Cox proportional hazards regression analysis indicated that younger age (adjusted hazard ratio [HR] = 3.166, 95% CI: 1.200–8.352, P = 0.021), larger tumor size (adjusted HR = 4.370, 95% CI: 1.671–11.428, P = 0.002), and multifocality/multicentricity (adjusted HR = 5.059, 95% CI: 2.166–11.818, P < 0.001) were independently associated with DFS.
Conclusion: Preoperative breast MRI features may be associated with ANB and DFS in patients with early-stage breast cancer.
Keywords: Breast neoplasms; Magnetic resonance imaging; Axilla; Lymph nodes; Survival

INTRODUCTION

With the widespread application of breast cancer screening

technology, the detection rate of early-stage breast cancer (cT1-2N0M0) has increased significantly [1]. Sentinel lymph node biopsy (SLNB) is the standard procedure for the axillary

evaluation of patients with early breast cancer [2]. Following the American College of Surgeons Oncology Group (ACOSOG) Z0011 trial, axillary lymph node (LN) evaluation focuses on the status of metastasis and the number of axillary LN metastases, known as the axillary nodal burden (ANB) [3,4]. High nodal burden (HNB), defined as the detection of three or more metastatic LNs, typically requires further axillary lymph node dissection (ALND), which patients with fewer than three metastatic LNs may be exempt from ALND [5]. However, if patients with HNB can be accurately identified before surgery, ALND can be performed without SLNB, reducing operation time and medical costs [6]. Furthermore, accurate preoperative prediction of HNB can alter the treatment strategy, allowing neoadjuvant therapy to downstage the axillary region and potentially avoid the need for ALND [7]. Therefore, precise preoperative prediction of ANB in early breast cancer is crucial for guiding clinical decision-making.

Current imaging techniques for assessing axillary LNs remain limited in terms of accuracy, even when combined with advanced detection equipment such as PET-CT [8], particularly in early-stage breast cancer, where metastatic LNs are often small [9]. Ultrasound (US) was the primary modality used to assess the axilla. However, its sensitivity and specificity nonpalpable LN evaluation range from 49% to 87% and 55% to 97%, respectively, influenced by operator dependence [8]. Potential primary breast tumor features in predicting axillary LN metastatic burden have been investigated [10-13]. Magnetic resonance imaging (MRI), a high-resolution multiparameter imaging technique, can provide comprehensive information on primary breast lesions [14]. Several studies have found that MRI features of primary breast cancer, such as edema, tumor size, and mass margins, are associated with ANB [5,15,16]. However, the findings of these studies were inconsistent. Additionally, the clinical significance of MRI signs not included in the lexicon of the American College of Radiology Breast Imaging and Reporting Data System (ACR BI-RADS), such as peritumoral edema and the adjacent vessel sign, is believed to be associated with lymphovascular invasion [17], a factor significantly linked to LN metastasis [18]. Therefore, further investigations are warranted to elucidate the predictive value of these MRI features for ANB. Moreover, the prognostic significance of MRI features of primary breast cancer in early-stage breast cancer remains poorly established.

Therefore, this study aimed to investigate whether MRI features of primary breast cancer can assist in predicting ANB and whether these imaging features are associated with disease-free survival (DFS) in patients with early-stage breast cancer.

MATERIALS AND METHODS

Study Population

This retrospective study was approved by the Institutional Ethics Review Board of Shanxi Province Cancer Hospital (IRB No. KY2022001), which waived the requirement for informed consent. Patients with early-stage breast cancer who underwent preoperative MRI at our hospital between December 2016 and December 2018 were retrospectively reviewed. The inclusion criteria were as follows: 1) patients who had pathologically confirmed invasive ductal carcinoma, and with clinical early-stage (cT1-2N0M0; tumor size ≤5 cm, no palpable axillary adenopathy, no metastasis), 2) patients who underwent preoperative breast MRI, 3) patients who underwent SLNB or ALND surgery within two weeks after the MRI examination. The exclusion criteria were as follows: 1) poor imaging quality, 2) patients with a history of other malignant tumors, 3) patients who received neoadjuvant chemotherapy before surgery, and 4) patients who underwent a primary breast cancer biopsy before the MRI examination. Based on the number of positive axillary LNs determined by postoperative pathology, patients were divided into the HNB (≥3 positive LNs) and non-HNB (<3 positive LNs) groups.

Breast MRI Examination

Breast MRI was performed with the patient in the prone position using a 3T system (Philips Achieva; Philips Healthcare, Best, the Netherlands) equipped with a dedicated 8-channel surface phased array breast coil. The routine protocol included turbo spin-echo T1-weighted (repetition time [ms]/echo time [ms], 4.5/1.98; field of view, 32 x 32 cm; matrix, 320 x 320; slice thickness, 1 mm) and T2-weighted fat-suppressed spin-echo sequences (3556/70; field of view, 32 x 32 cm; matrix, 456 x 364; slice thickness, 4 mm). Echoplanar diffusion-weighted imaging (DWI) was performed before contrast enhancement (8830/57; field of view, 32 x 32 cm; matrix, 128 x 126; slice thickness, 3 mm) with b-values of 0 and 1000 sec/mm^2. Dynamic contrast-enhanced MRI was performed using a T1-weighted gradient-echo sequence (3.9/1.84; field of view, 35 x 35 cm; matrix, 352 x 352; slice thickness, 2.5 mm). A total of 40 phases, each lasting 10.8 seconds, were scanned after the injection of a contrast agent. A bolus of 0.1 mmol/kg gadodiamide

(omniscan, GE Healthcare Ireland Limited, Cork, Ireland) was injected into the arm using high-pressure injectors at a rate of 3.0 mL/s, followed by a 20 mL saline flush.

Breast MRI Analysis

Two radiologists with 10 and 15 years, respectively, of experience in breast MRI independently reviewed the images. The original independent evaluations of the radiologists were recorded to calculate inter-reader agreement. For discrepancies, a consensus was reached through discussion. Only the largest lesion was quantitatively and qualitatively assessed for multifocal or multicentric lesions. The location and size of the lesions were recorded to ensure that both readers evaluated the same lesion. All images were evaluated using the 2013 Breast Imaging Reporting and Data System MR imaging lexicon [19]. The radiologists also evaluated the presence of 1) peritumoral edema, defined as higher signal intensity around the tumor on T2-weighted imaging (T2WI) compared to the surrounding breast tissue or similar to that of water (Supplementary Fig. 1A) [20], 2) prepectoral edema, defined as a water-like hyperintensity area with a linear or band-shaped extension to the pectoralis major muscle (Supplementary Fig. 1B) [21], 3) subcutaneous edema, defined as an intense water-like hyperintensity area extending to subcutaneous areas (Supplementary Fig. 1C) [21], 4) adjacent vascular signs, defined as the presence of blood vessels on contrast-enhanced T1WI that entered or touched the edge of the lesion [17], and 5) multifocality/multicentricity, defined as two or more highly suggestive malignant lesions (BI-RADS MRI 5) in the same or different quadrants, with normal breast parenchyma separating them. The assessment of highly suspicious malignant lesions was mainly based on dynamic contrast enhancement MRI, combined with DWI to ensure higher accuracy. Also assessed were 6) intratumoral necrosis, determined by a water-like hyperintensity area in the tumor on T2WI, without enhancement on DCE images [22], and 7) tumor apparent diffusion coefficient (ADC) value, calculated by placing three regions of interest ($\geq$20 mm^2) on different sections within the lesion on ADC images, avoiding necrotic areas with reference to T2WI and contrast-enhanced T1WI, and determining the average value as the ADC of each lesion. ADC values measured by senior radiologists were used for the analysis.

Pathological Evaluation

This study included preoperative clinical and pathological biopsy indicators such as age; menopausal status; histological grade; estrogen receptor (ER), progesterone receptor (PR), human epidermal growth factor receptor 2 (HER2), and Ki-67 expression status; and molecular subtype. ER or PR positivity was defined as $\geq$1% tumor nucleus staining, and the cutoff value for Ki-67 was 20%. For HER2 status, tumors with immunohistochemical (IHC) staining scores of 0 or 1+ and 3+ were defined as HER2-negative and HER2-positive, respectively, following American Society of Clinical Oncology/College of American Pathologists guidelines [23]. For tumors with an IHC staining score of 2+, fluorescence in situ hybridization (FISH) was performed to determine HER2 status. Non-amplified and amplified FISH results indicated HER2-negative and HER2-positive tumors, respectively. According to the 2013 St. Gallen conference, breast cancer was classified into four molecular subtypes: luminal A, luminal B, HER2-enriched, and triple-negative subtype [24].

Follow-Up

The endpoint of this study was DFS, defined as the time from the date of surgery to the first local recurrence, distant metastasis, or death from any cause, whichever occurred first. Patients were followed up postoperatively with physical examination, chest CT, and breast and abdominal US every 3–6 months for the first 2 years and then annually according to the follow-up protocol of our institution. Bone scanning and PET-CT were performed if necessary. Recurrence or metastasis was confirmed using imaging or histopathology. Follow-up began on the first day after surgery and ended in June 2022. Patients who did not experience recurrence, distant metastasis, or death at the last follow-up or those who were lost to follow-up were excluded from the analysis.

Statistical Analysis

Statistical analyses were performed using statistical software (SPSS version 22.0, IBM Corp., Armonk, NY, USA; MedCalc version 19.6.4, MedCalc Software Ltd., Ostend, Belgium; and X-Tile version 3.6.1, Yale University, New Haven, CT, USA). Statistical significance was set at $P <$ 0.05. significant. Differences in the clinicopathological characteristics and MRI features of primary breast cancer between the HNB and non-HNB groups were compared using the Student's t-test, Mann-Whitney U-test, χ^2 test, or Fisher exact test, as appropriate. Univariable and multivariable logistic regression analyses were conducted to identify independent risk factors associated with HNB. Variables

with $P < 0.05$ in the univariable analyses were entered into the multivariable analyses. The predictive efficacy of the identified risk factors for HNB was evaluated using the receiver operating characteristic (ROC) curve and area under the curve (AUC). The inter-reader agreement was evaluated for each variable, using the kappa test and intraclass correlation coefficient for qualitative and quantitative variables, respectively. Univariable and multivariable Cox proportional hazards regression analyses were performed to determine whether the preoperative clinicopathological characteristics and MRI features of primary breast cancer were related to DFS. Adjusted Kaplan-Meier survival curves were generated to illustrate the impact of significant risk factors identified by multivariable Cox proportional hazards regression analysis [25]. Variables with $P < 0.1$ in the univariable Cox analyses were entered into the multivariable Cox analyses. The X-Tile program was used to select the optimum cutoff for continuous variables according to the highest χ^2 value defined by Kaplan-Meier survival analysis and log-rank test [26].

RESULTS

Clinical-Pathologic Characteristics and Preoperative Breast MRI Features

Among the initial cohort of 453 patients, 156 individuals were excluded, resulting in a sample of 297 female patients, aged 23–76 years (mean 50 ± 10) (Fig. 1). There were 47 and 250 patients in the HNB (range, 3–32 positive LNs) and non-HNB (range, 0–2 positive LNs) groups, respectively. The clinicopathological characteristics of the HNB and non-HNB groups are compared in Table 1. No significant differences were observed in age, menopausal status, ER, PR, HER2, Ki-67, molecular subtype, or pathological grade between the two groups (all $P > 0.05$). However, significant differences were noted in tumor size, lesion type, multifocality or multicentricity, adjacent vessel signs, peritumoral edema, and subcutaneous edema (all $P < 0.05$) (Table 2). Regarding the breast MRI features, satisfactory concordance existed between the two radiologists, as evidenced by κ values or intraclass correlation coefficients ranging from 0.757 to 0.966 (Supplementary Table 1).

Association Between Preoperative Breast MRI Features and HNB

Univariable analysis showed that tumor size on MRI, adjacent vessel sign, NME lesion type, multifocality/multicentricity, peritumoral edema, and subcutaneous edema were significantly correlated with HNB (Supplementary Table 2). Multivariable logistic regression showed that multifocality/multicentricity (adjusted OR = 3.905, 95% CI: 1.685–9.051, $P = 0.001$) and peritumoral edema (adjusted OR = 3.734, 95% CI: 1.644–8.479, $P = 0.002$) were independent risk factors for HNB (Supplementary Table 2, Figs. 2, 3). Regarding the predictive value of HNB, the AUCs for peritumoral edema and multifocality/multicentricity were 0.719 (95% CI: 0.664–0.769) and 0.622 (95% CI: 0.564–0.678), respectively. Combined peritumoral
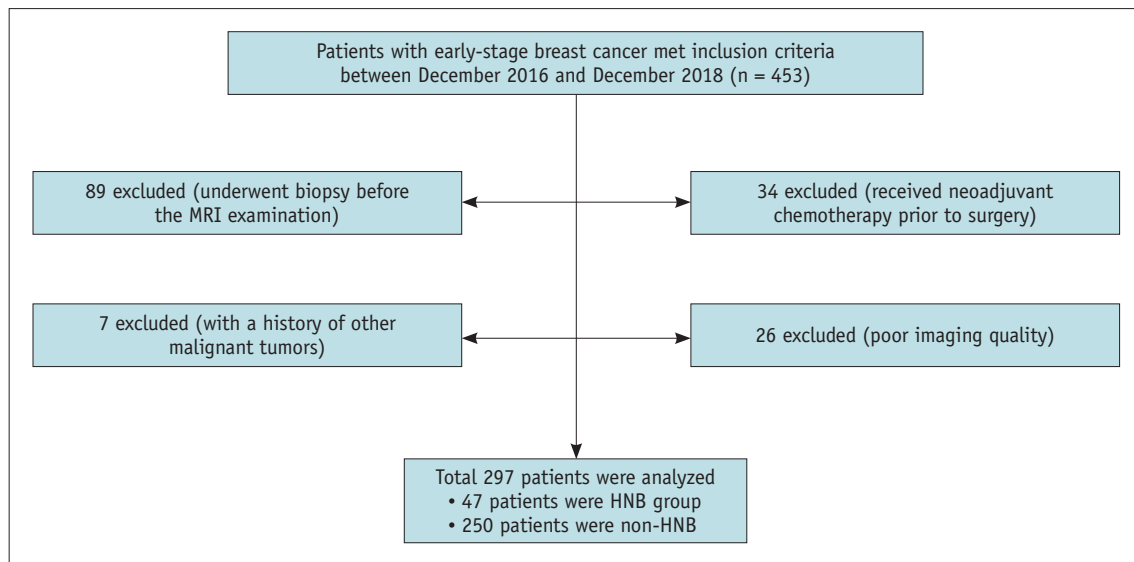
Fig. 1. Flowchart of the study patients. HNB = high nodal burden

edema and multifocality/multicentricity achieved an AUC of 0.760 (95% CI: 0.707–0.807), which was higher than that of any single factor (*P* = 0.011 and *P* = 0.001, respectively). The sensitivity and specificity at the optimal threshold according to the Youden index (0.462) were 83.0% and 63.2%, respectively.

Association Between Preoperative Breast MRI Features and DFS

The median follow-up period was 45 months (range, 5–61 months). Disease relapse occurred in 26 of the 297 patients (8.75%) during a median follow-up period of 24 months (range, 5–41 months). Among these 26 patients, 17 (65.38%) had distant metastasis (bone [n = 8], lung [n = 4], liver [n = 4], and brain [n = 1]), 2 (7.69%) had local recurrence (ipsilateral chest wall), and 7 (26.93%) had both distant metastasis and local recurrence (ipsilateral

Table 1. Comparison of clinicopathological characteristics between HNB group and Non-HNB group

Characteristics	Non-HNB (n = 250)	HNB (n = 47)	*P*
Age, yrs	49.87 ± 9.94	50.15 ± 9.45	0.858
Menopausal status			0.487
Premenopausal	146 (58.4)	30 (63.8)	
Postmenopausal	104 (41.6)	17 (36.2)	
ER status			0.374
Negative	63 (25.2)	9 (19.1)	
Positive	187 (74.8)	38 (80.9)	
PR status			0.505
Negative	98 (39.2)	16 (34.0)	
Positive	152 (60.8)	31 (66.0)	
HER2 status			0.411
Negative	194 (77.6)	39 (83.0)	
Positive	56 (22.4)	8 (17.0)	
Ki-67 index			0.948
<20%	68 (27.2)	13 (27.7)	
≥20%	182 (72.8)	34 (72.3)	
Molecular subtype			0.528
Luminal A	64 (25.6)	12 (25.5)	
Luminal B	125 (50.0)	26 (55.3)	
HER2 enriched	26 (10.4)	6 (12.8)	
Triple-negative	35 (14.0)	3 (6.4)	
Histologic grade			0.667
Low and moderate	184 (73.6)	36 (76.6)	
High	66 (26.4)	11 (23.4)	

Data are number of patients with percentage in parentheses, except for age presented as mean ± standard deviation.
HNB = high nodal burden, ER = estrogen receptor, PR = progesterone receptor, HER2 = human epidermal growth factor receptor 2

Table 2. Comparison of preoperative breast MRI features between HNB group and non-HNB group

Features	Non-HNB (n = 250)	HNB (n = 47)	*P*
All (n = 297)			
Tumor size on MRI, cm	1.8 (1.4–2.3)	2.4 (1.8–3.6)	<0.001*
Lesion type			0.004†
Mass	236 (94.4)	38 (80.9)	
NME	14 (5.6)	9 (19.1)	
TIC pattern			0.513†
Type I	9 (3.6)	0 (0)	
Type II	147 (58.8)	30 (63.8)	
Type III	94 (37.6)	17 (36.2)	
Intratumoral necrosis			0.392†
Negative	227 (90.8)	45 (95.7)	
Positive	23 (9.2)	2 (4.3)	
Multifocality/multicentricity			<0.001
Negative	226 (90.4)	31 (66.0)	
Positive	24 (9.6)	16 (34.0)	
Adjacent vessel sign			0.003
Negative	215 (86.0)	32 (68.1)	
Positive	35 (14.0)	15 (31.9)	
Peritumoral edema			<0.001
Negative	168 (67.2)	11 (23.4)	
Positive	82 (32.8)	36 (76.6)	
Prepectoral edema			0.090†
Negative	232 (92.8)	40 (85.1)	
Positive	18 (7.2)	7 (14.9)	
Subcutaneous edema			0.001†
Negative	247 (98.8)	41 (87.0)	
Positive	3 (1.2)	6 (13.0)	
Tumor ADC, x 10^{-3} mm^2/s	0.831 ± 0.142	0.818 ± 0.143	0.580
Mass (n = 274)			
Shape			0.103
Oval or round	44 (18.6)	3 (7.9)	
Irregular	192 (81.4)	35 (92.1)	
Margin			0.778†
Circumscribed	25 (10.6)	3 (7.9)	
Not circumscribed	211 (89.4)	35 (92.1)	
Internal enhancement			0.266
Rim enhancement	42 (17.8)	4 (10.5)	
Others	194 (82.2)	34 (89.5)	
NME (n = 23)			
Distribution			1.000†
Linear or segmental	8 (57.1)	6 (66.7)	
Others	6 (42.9)	3 (33.3)	
Internal enhancement			1.000†
Clustered ring	6 (42.9)	3 (33.3)	
Others	8 (57.1)	6 (66.7)	

Data are number of patients with percentage in parentheses, except for tumor size on MRI presented as medians with interquartile ranges in parentheses, and tumor ADC presented as mean ± standard deviation.
*P*-values were obtained with the Mann-Whitney U test, †*P*-values were obtained with the Fisher exact test. Unless otherwise specified, continuous variables were compared by the Student *t*-test, and categorical variables were compared using the χ^2 test.
HNB = high nodal burden, NME = non-mass enhancement, TIC = time-intensity curve, ADC = apparent diffusion coefficient
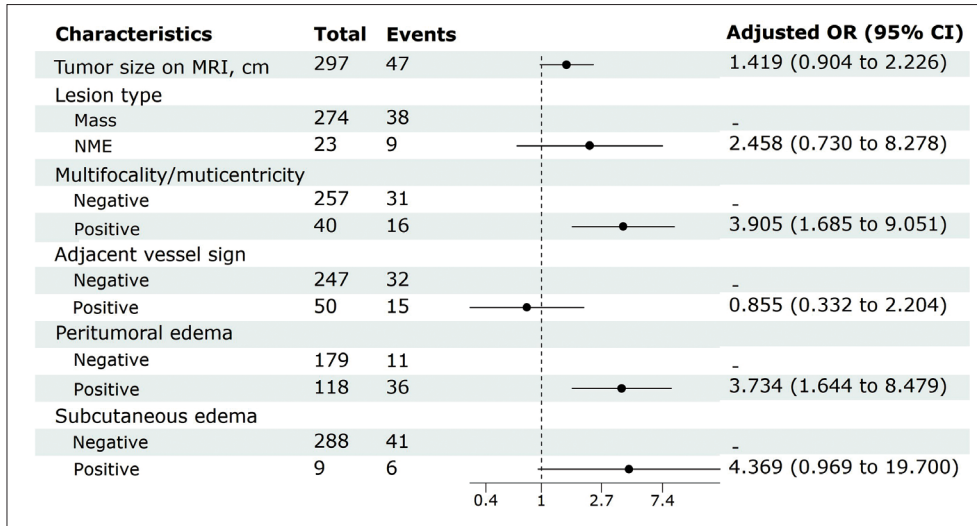
chest wall and bone [n = 3], ipsilateral chest wall and lung [n = 2], ipsilateral chest wall and mediastinal LN [n = 1], supraclavicular and cervical LN [n = 1]). Four patients died during the treatment for metastasis. The optimum cutoff values for age, tumor size, and ADC were 52 years, 2.1 cm, and 0.990×10^{-3} mm^2/s, respectively. Univariable and multivariable Cox regression analyses of preoperative clinicopathological characteristics and MRI features of primary breast cancer associated with DFS in patients with early-stage breast cancer are presented in Supplementary Table 3. Younger age (≤52) (adjusted hazard ratio [HR] = 3.166, 95% CI: 1.200–8.352, $P = 0.021$), larger tumor size (>2.1 cm) (adjusted HR = 4.370, 95% CI: 1.671–11.428, $P = 0.002$) and presence of multifocality/multicentricity (adjusted HR = 5.059, 95% CI: 2.166–11.818, $P < 0.001$) were independently associated with poor DFS (Supplementary Table 3, Figs. 4, 5).
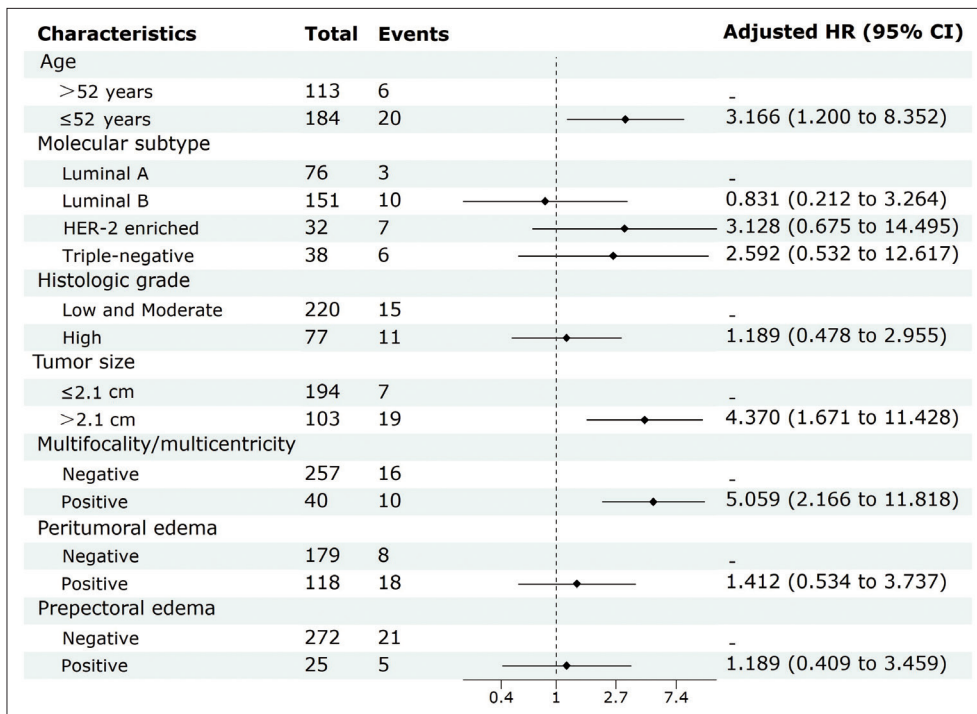
DISCUSSION

Preoperative prediction of HNB may avoid the underestimation of LN staging using SLNB alone [8]. Furthermore, it may modify treatment strategy, allowing neoadjuvant therapy to downstage the axillary region and potentially avoid ALND [8]. In this study, we investigated the MRI features of primary breast cancer to predict ANB in patients with early-stage breast cancer. Peritumoral edema and multifocal/multicentricity on MRI were independent risk factors for HNB. Additionally, age, tumor size, and multifocal/multicentricity on MRI were associated with DFS, thus being crucial in predicting the prognosis of patients with early-stage breast cancer before surgery. The predictors identified in this study are easily obtainable through routine examinations and can aid in tailoring personalized therapeutic regimens and evaluating the prognosis of patients with early-stage breast cancer.
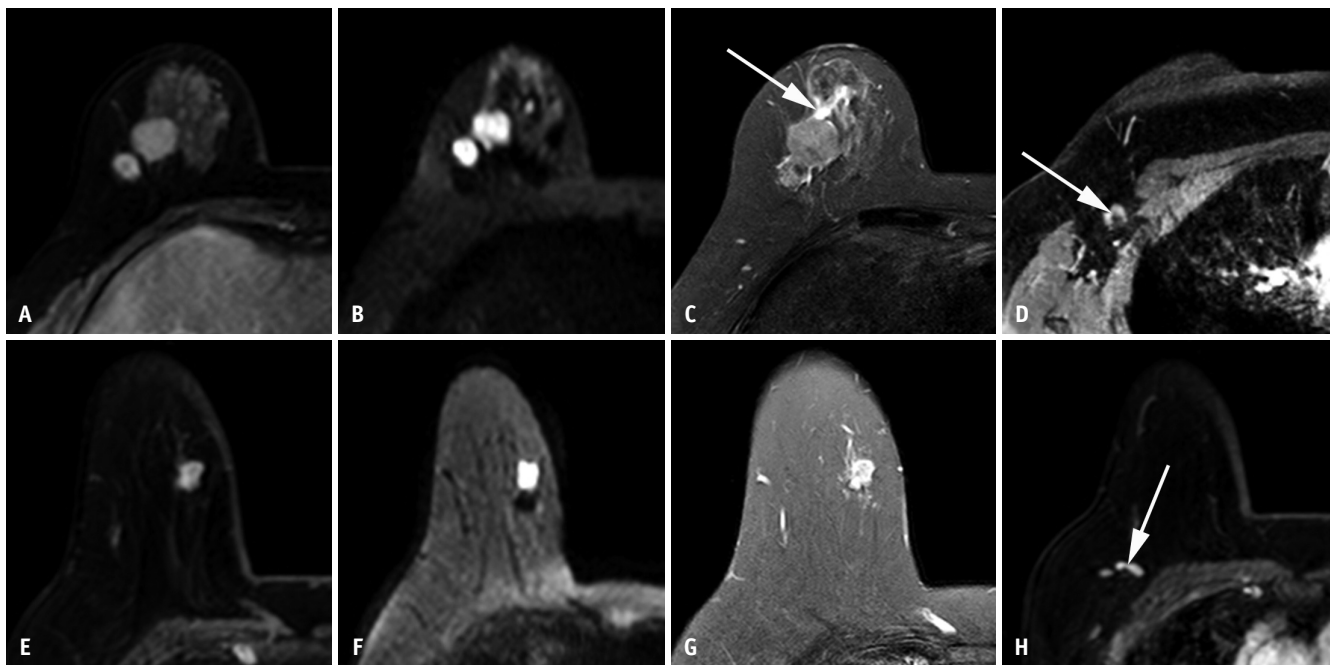
Fig. 2. Representative MR images of HNB and non-HNB patients with early-stage breast cancer. **A-D:** 62-year-old female with invasive ductal carcinoma of the right breast. **(A)** Contrast-enhanced T1WI shows two masses (22 mm and 11 mm) in the lower outer quadrant of the right breast, with irregular margins and heterogeneous/rim enhancement. **(B)** DWI shows high signal intensity in both nodes, with similar ADC values (0.855×10^{-3} mm^2/s and 0.827×10^{-3} mm^2/s, respectively). It is considered multifocal breast cancer. **(C)** Fat-suppressed T2WI shows high-signal around the tumor, which represents peritumoral edema (arrow). **(D)** The right axilla shows a slightly enlarged lymph node (9 mm x 4 mm) with a central fatty hilum (arrow). The patient has four metastatic lymph nodes confirmed by pathology and is classified as HNB. **E-H:** 63-year-old female with invasive ductal carcinoma of the right breast. **(E)** Contrast-enhanced T1WI shows a single mass (14 mm) with irregular margins and heterogeneous enhancement in the upper inner quadrant of the right breast. **(F)** DWI shows high signal intensity, with ADC values of 0.743×10^{-3} mm^2/s. **(G)** Fat-suppressed T2WI shows no peritumoral edema. **(H)** The right axilla shows a slightly enlarged lymph node (13 mm x 4 mm) with a homogeneous C-shaped cortex (arrow). The patient has one pathologically confirmed metastatic lymph node and is classified as non-HNB. HNB = high nodal burden, WI = weighted imaging, DWI = diffusion weighted imaging, ADC = apparent diffusion coefficient

| Characteristics	Total	Events		Adjusted OR (95% CI)
Tumor size on MRI, cm	297	47		1.419 (0.904 to 2.226)
Lesion type				
Mass	274	38		-
NME	23	9		2.458 (0.730 to 8.278)
Multifocality/muticentricity				
Negative	257	31		-
Positive	40	16		3.905 (1.685 to 9.051)
Adjacent vessel sign				
Negative	247	32		-
Positive	50	15		0.855 (0.332 to 2.204)
Peritumoral edema				
Negative	179	11		-
Positive	118	36		3.734 (1.644 to 8.479)
Subcutaneous edema				
Negative	288	41		-
Positive	9	6		4.369 (0.969 to 19.700)

0.4   1   2.7   7.4

Fig. 3. Forest plot of multivariable logistic regression analyses of the preoperative clinicopathological characteristics and MRI features associated with high nodal burden for early-stage breast cancer. OR = odds ratio, CI = confidence interval, NME = non-mass enhancement

Characteristics	Total	Events		Adjusted HR (95% CI)
Age				
>52 years	113	6		-
≤52 years	184	20		3.166 (1.200 to 8.352)
Molecular subtype				
Luminal A	76	3		-
Luminal B	151	10		0.831 (0.212 to 3.264)
HER-2 enriched	32	7		3.128 (0.675 to 14.495)
Triple-negative	38	6		2.592 (0.532 to 12.617)
Histologic grade				
Low and Moderate	220	15		-
High	77	11		1.189 (0.478 to 2.955)
Tumor size				
≤2.1 cm	194	7		-
>2.1 cm	103	19		4.370 (1.671 to 11.428)
Multifocality/multicentricity				
Negative	257	16		-
Positive	40	10		5.059 (2.166 to 11.818)
Peritumoral edema				
Negative	179	8		-
Positive	118	18		1.412 (0.534 to 3.737)
Prepectoral edema				
Negative	272	21		-
Positive	25	5		1.189 (0.409 to 3.459)

0.4   1   2.7   7.4

Fig. 4. Forest plot of multivariable adjusted Cox regression analyses of the preoperative clinicopathological characteristics and MRI features associated with disease-free survival for early-stage breast cancer patients. HR = hazard ratio, CI = confidence interval, HER2 = human epidermal growth factor receptor 2

The fifth edition of the BI-RADS is commonly employed to evaluate breast MRI, focusing primarily on the dynamic contrast-enhancement characteristics of breast lesions. Peritumoral edema observed on breast T2WI MRI is often overlooked by radiologists given its exclusion from the BI-RADS lexicon. Nevertheless, several studies have demonstrated its correlation with certain pathological indicators and prognosis [17,27,28]. In the present study, the incidence of peritumoral edema was significantly higher in the HNB than in the non-HNB group. Multivariable logistic regression demonstrated that peritumoral edema was a predictor of HNB in early breast cancer, which is
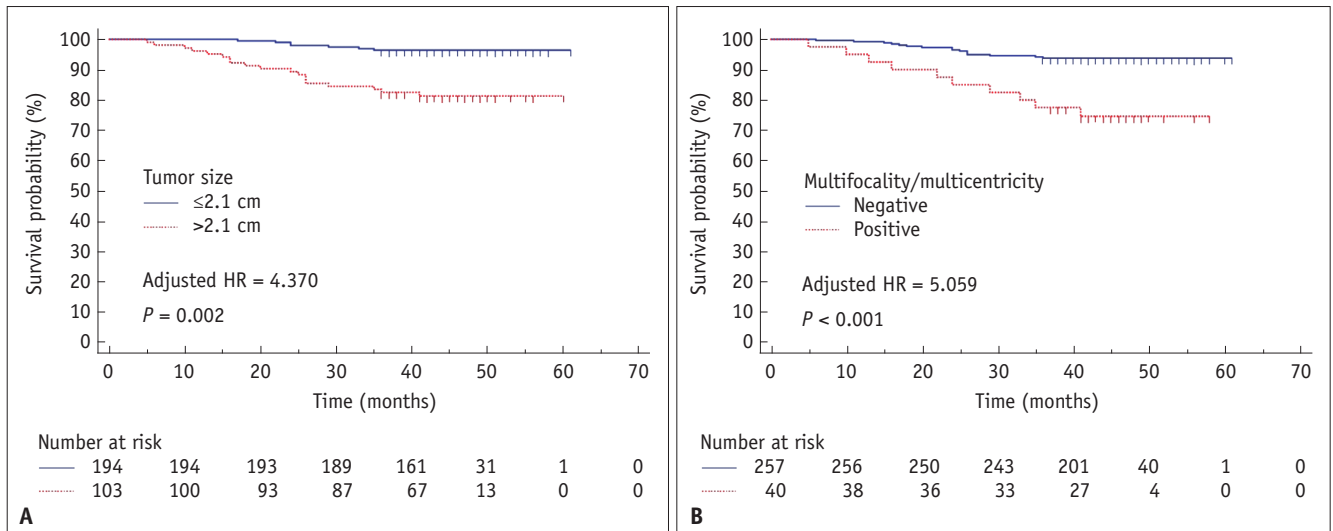
Fig. 5. Adjusted Kaplan-Meier survival curves of disease-free survival according to **(A)** tumor size (adjusted HR = 4.370, 95% CI: 1.671–11.428, *P* = 0.002) and **(B)** multifocality/multicentricity (adjusted HR = 5.059, 95% CI: 2.166–11.818, *P* < 0.001) on preoperative breast MRI in patients with early-stage breast cancer. HR = hazard ratio, CI = confidence interval

consistent with previous studies [15,20]. However, the exact biological mechanisms underlying the formation of peritumoral edema remain unclear. Baltzer et al. [29] suggested that more invasive tumors are often surrounded by increased angiogenesis and newly formed immature blood vessels given their higher permeability. These tumors easily cause vasogenic edema, which manifests as a high signal on peritumoral T2WI. Koyama et al. [30] proposed that highly malignant breast cancers tend to secrete abundant hyaluronidase, which induces the degradation of neighboring tissues, facilitating the shedding and colonization of cancer cells. Interstitial hyaluronidase, which prolongs T2 relaxation time, leads to a high signal area on T2WI. These findings collectively support the notion that breast cancers with peritumoral edema tend to exhibit greater aggressiveness and metastasis, resulting in greater LN metastatic burden.

Multifocal or multicentric breast cancer has been reported to occur in approximately 21%–63% of cases [31]. Owing to its high sensitivity in breast cancer detection and ability to identify occult cancer foci undetectable by other imaging modalities, MRI has become the recommended technique for detecting multifocal or multicentric breast cancer [14]. In this study, multifocality or multicentricity on breast MRI was an independent risk factor for HNB in early-stage breast cancer. Previous studies have shown that multifocal or multicentric breast cancer is associated with a higher incidence of axillary LN metastasis, which may be attributed to its biologically more aggressive nature than unifocal breast cancer [32,33]. Multifocal and multicentric breast

cancers also tend to have a higher total tumor burden, facilitating axillary LN metastasis and local recurrence [34].

In this study, tumor size observed on MRI was a significant prognostic factor for DFS in early breast cancer. X-tile plots indicated that a cutoff value of 2.1 cm was optimal, which is approximately equivalent to the demarcation between the T1 and T2 stages in the American Joint Committee on Cancer staging system [35]. Therefore, early T-staging remains an important prognostic factor for early-stage breast cancer. Additionally, multifocality or multicentricity observed on MRI was associated with prognosis, which is consistent with the findings of Bitencourt et al. [36], whose study revealed that multifocality identified through MRI had prognostic significance, whereas the same features identified through postoperative pathology did not. Bitencourt et al. [36] suggested that smaller lesions may be missed in pathological sections and that the administration of chemotherapy could complicate the detection of multifocality. In summary, the previously overlooked presence of multiple foci on MRI may be valuable in prognostic assessment but requires additional research.

Our study had several limitations. First, patient selection bias was inevitable given its retrospective design. Second, since this was a single-center study, further validation from other research institutions is required. Third, our study explored only the MRI features of primary tumors relative to HNB and DFS. The incorporation of primary breast tumors and axillary features warrants further investigation. Finally, the median follow-up duration of 45 months was relatively

short to evaluate DFS. We will continue to monitor the survival of these patients.

In conclusion, our study demonstrates that multifocality/multicentricity and peritumoral edema observed on MRI can help predict a HNB in patients with early breast cancer. Furthermore, younger age, larger tumor size, and multifocality/multicentricity on MRI were associated with worse DFS. Therefore, preoperative MRI may assist in treatment decision-making and prognostic evaluation for patients with early breast cancer.

Supplement

The Supplement is available with this article at https://doi.org/10.3348/kjr.2024.0196.

Availability of Data and Material

The datasets generated or analyzed during the study are available from the corresponding author on reasonable request.

Conflicts of Interest

The authors have no potential conflicts of interest to disclose.

Author Contributions

Conceptualization: Junjie Zhang, Zhi Yin. Data curation: Jianxin Zhang, Ruirui Song. Formal analysis: Junjie Zhang, Zhi Yin. Funding acquisition: Yanfen Cui, Xiaotang Yang. Investigation: Jianxin Zhang, Ruirui Song. Methodology: Junjie Zhang. Project administration: Yanfen Cui, Xiaotang Yang. Resources: Jianxin Zhang. Software: Zhi Yin. Supervision: Yanfen Cui, Xiaotang Yang. Validation: Junjie Zhang, Zhi Yin. Visualization: Junjie Zhang, Zhi Yin. Writing—original draft: Junjie Zhang, Zhi Yin. Writing—review & editing: all authors.

ORCID IDs

Junjie Zhang
    https://orcid.org/0000-0001-9102-6588
Zhi Yin
    https://orcid.org/0009-0004-3253-4522
Jianxin Zhang
    https://orcid.org/0000-0002-7062-0972
Ruirui Song
    https://orcid.org/0000-0002-3393-2985
Yanfen Cui
    https://orcid.org/0000-0001-6631-5687
Xiaotang Yang
    https://orcid.org/0000-0002-2233-1404

Funding Statement

REFERENCES

1. Higgins T, Mittendorf EA. Peritumoral lidocaine injection: a low-cost, easily implemented intervention to improve outcomes in early-stage breast cancer. *J Clin Oncol* 2023;41:3287-3290
2. Boughey JC, Ballman KV, Hunt KK, McCall LM, Mittendorf EA, Ahrendt GM, et al. Axillary ultrasound after neoadjuvant chemotherapy and its impact on sentinel lymph node surgery: results from the American College of Surgeons Oncology Group Z1071 trial (Alliance). *J Clin Oncol* 2015;33:3386-3393
3. Giuliano AE, Hunt KK, Ballman KV, Beitsch PD, Whitworth PW, Blumencranz PW, et al. Axillary dissection vs no axillary dissection in women with invasive breast cancer and sentinel node metastasis: a randomized clinical trial. *JAMA* 2011;305:569-575
4. Lim GH, Upadhyaya VS, Acosta HA, Lim JMA, Allen JC Jr, Leong LCH. Preoperative predictors of high and low axillary nodal burden in Z0011 eligible breast cancer patients with a positive lymph node needle biopsy result. *Eur J Surg Oncol* 2018;44:945-950
5. Kim WH, Kim HJ, Lee SM, Cho SH, Shin KM, Lee SY, et al. Prediction of high nodal burden with ultrasound and magnetic resonance imaging in clinically node-negative breast cancer patients. *Cancer Imaging* 2019;19:4
6. Lim GH, Teo SY, Allen JC Jr, Chinthala JP, Leong LCH. Determining whether high nodal burden in early breast cancer patients can be predicted preoperatively to avoid sentinel lymph node biopsy. *J Breast Cancer* 2019;22:67-76
7. Pilewskie M, Morrow M. Axillary nodal management following neoadjuvant chemotherapy: a review. *JAMA Oncol* 2017;3:549-555
8. Chang JM, Leung JWT, Moy L, Ha SM, Moon WK. Axillary nodal evaluation in breast cancer: state of the art. *Radiology* 2020;295:500-515

9. Kuijs VJ, Moossdorff M, Schipper RJ, Beets-Tan RG, Heuts EM, Keymeulen KB, et al. The role of MRI in axillary lymph node imaging in breast cancer patients: a systematic review. *Insights Imaging* 2015;6:203-215

10. Yi CB, Ding ZY, Deng J, Ye XH, Chen L, Zong M, et al. Combining the ultrasound features of primary tumor and axillary lymph nodes can reduce false-negative rate during the prediction of high axillary node burden in BI-RADS category 4 or 5 breast cancer lesions. *Ultrasound Med Biol* 2020;46:1941-1948

11. Li JW, Tong YY, Jiang YZ, Shui XJ, Shi ZT, Chang C. Clinicopathologic and ultrasound variables associated with a heavy axillary nodal tumor burden in invasive breast carcinoma. *J Ultrasound Med* 2019;38:1747-1755

12. Dihge L, Bendahl PO, Rydén L. Nomograms for preoperative prediction of axillary nodal status in breast cancer. *Br J Surg* 2017;104:1494-1505

13. Zhao F, Cai C, Liu M, Xiao J. Identification of the lymph node metastasis-related automated breast volume scanning features for predicting axillary lymph node tumor burden of invasive breast cancer via a clinical prediction model. *Front Endocrinol (Lausanne)* 2022;13:881761

14. Mann RM, Cho N, Moy L. Breast MRI: state of the art. *Radiology* 2019;292:520-536

15. Xu Z, Ding Y, Zhao K, Han C, Shi Z, Cui Y, et al. MRI characteristics of breast edema for assessing axillary lymph node burden in early-stage breast cancer: a retrospective bicentric study. *Eur Radiol* 2022;32:8213-8225

16. Li J, Ma W, Jiang X, Cui C, Wang H, Chen J, et al. Development and validation of nomograms predictive of axillary nodal status to guide surgical decision-making in early-stage breast cancer. *J Cancer* 2019;10:1263-1274

17. Cheon H, Kim HJ, Lee SM, Cho SH, Shin KM, Kim GC, et al. Preoperative MRI features associated with lymphovascular invasion in node-negative invasive breast cancer: a propensity-matched analysis. *J Magn Reson Imaging* 2017;46:1037-1044

18. Zhang S, Zhang D, Yi S, Gong M, Lu C, Cai Y, et al. The relationship of lymphatic vessel density, lymphovascular invasion, and lymph node metastasis in breast cancer: a systematic review and meta-analysis. *Oncotarget* 2017;8:2863-2873

19. D'Orsi CJ, Sickles EA, Mendelson EB, Morris EA. *ACR BI-RADS atlas: breast imaging reporting and data system*. 5th ed. Reston: American College of Radiology, 2013

20. Byon JH, Park YV, Yoon JH, Moon HJ, Kim EK, Kim MJ, et al. Added value of MRI for invasive breast cancer including the entire axilla for evaluation of high-level or advanced axillary lymph node metastasis in the post-ACOSOG Z0011 trial era. *Radiology* 2021;300:46-54

21. Harada TL, Uematsu T, Nakashima K, Sugino T, Nishimura S, Takahashi K, et al. Is the presence of edema and necrosis on T2WI pretreatment breast MRI the key to predict pCR of triple negative breast cancer? *Eur Radiol* 2020;30:3363-3370

22. Abdelhafez AH, Musall BC, Adrada BE, Hess K, Son JB, Hwang KP, et al. Tumor necrosis by pretreatment breast MRI: association with neoadjuvant systemic therapy (NAST)

response in triple-negative breast cancer (TNBC). *Breast Cancer Res Treat* 2021;185:1-12

23. Wolff AC, Hammond MEH, Allison KH, Harvey BE, Mangu PB, Bartlett JMS, et al. Human epidermal growth factor receptor 2 testing in breast cancer: American Society of Clinical Oncology/College of American Pathologists clinical practice guideline focused update. *J Clin Oncol* 2018;36:2105-2122

24. Goldhirsch A, Winer EP, Coates AS, Gelber RD, Piccart-Gebhart M, Thürlimann B, et al. Personalizing the treatment of women with early breast cancer: highlights of the St Gallen international expert consensus on the primary therapy of early breast cancer 2013. *Ann Oncol* 2013;24:2206-2223

25. Park SH, Han K, Park SY. Mistakes to avoid for accurate and transparent reporting of survival analysis in imaging research. *Korean J Radiol* 2021;22:1587-1593

26. Camp RL, Dolled-Filhart M, Rimm DL. X-tile: a new bio-informatics tool for biomarker assessment and outcome-based cut-point optimization. *Clin Cancer Res* 2004;10:7252-7259

27. Cheon H, Kim HJ, Kim TH, Ryeom HK, Lee J, Kim GC, et al. Invasive breast cancer: prognostic value of peritumoral edema identified at preoperative MR imaging. *Radiology* 2018;287:68-75

28. Kwon BR, Shin SU, Kim SY, Choi Y, Cho N, Kim SM, et al. Microcalcifications and peritumoral edema predict survival outcome in luminal breast cancer treated with neoadjuvant chemotherapy. *Radiology* 2022;304:310-319

29. Baltzer PA, Yang F, Dietzel M, Herzog A, Simon A, Vag T, et al. Sensitivity and specificity of unilateral edema on T2w-TSE sequences in MR-mammography considering 974 histologically verified lesions. *Breast J* 2010;16:233-239

30. Koyama H, Kobayashi N, Harada M, Takeoka M, Kawai Y, Sano K, et al. Significance of tumor-associated stroma in promotion of intratumoral lymphangiogenesis: pivotal role of a hyaluronan-rich tumor microenvironment. *Am J Pathol* 2008;172:179-193

31. Song SE, Park EK, Cho KR, Seo BK, Woo OH, Jung SP, et al. Additional value of diffusion-weighted imaging to evaluate multifocal and multicentric breast cancer detected using pre-operative breast MRI. *Eur Radiol* 2017;27:4819-4827

32. Grimm LJ, Johnson KS, Marcom PK, Baker JA, Soo MS. Can breast cancer molecular subtype help to select patients for preoperative MR imaging? *Radiology* 2015;274:352-358

33. Weissenbacher TM, Zschage M, Janni W, Jeschke U, Dimpfl T, Mayr D, et al. Multicentric and multifocal versus unifocal breast cancer: is the tumor-node-metastasis classification justified? *Breast Cancer Res Treat* 2010;122:27-34

34. Fushimi A, Yoshida A, Yagata H, Takahashi O, Hayashi N, Suzuki K, et al. Prognostic impact of multifocal and multicentric breast cancer versus unifocal breast cancer. *Surg Today* 2019;49:224-230

35. Giuliano AE, Edge SB, Hortobagyi GN. Eighth edition of the AJCC cancer staging manual: breast cancer. *Ann Surg Oncol* 2018;25:1783-1785

36. Bitencourt AGV, Eugênio DSG, Souza JA, Souza JO, Makdissi FBA, Marques EF, et al. Prognostic significance of preoperative MRI findings in young patients with breast cancer. *Sci Rep* 2019;9:3106